*diversity*

MDPI

*Article*

# Land Use and Land Cover Trends and Their Impact on Streamflow and Sediment Yield in a Humid Basin of Brazil's Atlantic Forest Biome

**Jussara Freire de Souza Viana [1], Suzana Maria Gico Lima Montenegro [1], Raghavan Srinivasan [2], Celso Augusto Guimarães Santos [3,*], Manoranjan Mishra [4], Ahmed Mukalazi Kalumba [5] and Richarde Marques da Silva [6]**

1 Department of Civil and Environmental Engineering, Federal University of Pernambuco, Recife 50740-530, Brazil; jussarafsouza@yahoo.com.br (J.F.d.S.V.); suzanam@ufpe.br (S.M.G.L.M.)
2 Department of Ecosystem Science and Management and Biological and Agricultural Engineering, Spatial Sciences Laboratory, Texas A&M University, College Station, TX 77843, USA; r-srinivasan@tamu.edu
3 Department of Civil and Environmental Engineering, Federal University of Paraíba, João Pessoa 58051-900, Brazil
4 Department of Geography, Fakir Mohan University, Vyasa Vihar, Nuapadhi, Balasore 756020, India; geo.manu05@gmail.com
5 Department of Geography and Environmental Science, Faculty of Science and Agriculture, University of Fort Hare, Alice 5700, South Africa; akalumba@ufh.ac.za
6 Department of Geosciences/CCEN, Federal University of Paraíba, João Pessoa 58051-900, Brazil; richarde@geociencias.ufpb.br
* Correspondence: celso@ct.ufpb.br; Tel.: +55-83-3216-7684

**Abstract:** Understanding the trends in land use and land cover (LULC) is crucial for modeling streamflow and sediment yield, particularly in hydrological basins. This study examined the impact of LULC on the dynamics of streamflow and sediment yield within a humid tropical basin of the Atlantic Forest biome in Brazil, focusing on the period from 2000 to 2016. Changes in LULC were analyzed using annual MapBiomas data products for the same period. The Soil and Water Assessment Tool (SWAT) model was deployed to simulate streamflow and sediment yield based on LULC changes. To investigate temporal trends in LULC, a suite of non-parametric statistical tests, including the Mann–Kendall, Pettitt, and Sen's slope estimator tests, was employed. Ecological diversity indices such as Shannon–Weaver, Simpson, and Pielou were applied to assess forest fragmentation, along with the Forest Fragmentation Index. The results revealed a growing trend in urban and sugarcane areas, coupled with a decline in dense vegetation, mangroves, and other forms of dense vegetation. With regard to the correlation between land uses and hydrological variables, the findings indicate minor variations in hydrological balance, attributable to the not-so-significant changes among the studied land-use scenarios, except for sediment yield estimates, which showed more considerable alterations. Notably, the estimates for 2000 and 2013–2016 were the most divergent. In a broader scientific context, this research conclusively establishes that the incorporation of dynamic LULC data into the SWAT model augments the precision and robustness of simulations pertaining to agricultural watersheds, thereby enabling a more comprehensive hydrological characterization of the study area.

**Keywords:** vegetation monitoring; MapBiomas; hydrological modeling; SWAT model; sediment yield

check for updates

**Citation:** Viana, J.F.d.S.; Montenegro, S.M.G.L.; Srinivasan, R.; Santos, C.A.G.; Mishra, M.; Kalumba, A.M.; da Silva, R.M. Land Use and Land Cover Trends and Their Impact on Streamflow and Sediment Yield in a Humid Basin of Brazil's Atlantic Forest Biome. *Diversity* **2023**, *15*, 1220. https://doi.org/10.3390/d15121220

Academic Editor: Mario A. Pagnotta

Received: 7 November 2023
Revised: 11 December 2023
Accepted: 13 December 2023
Published: 16 December 2023

**Copyright:** © 2023 by the authors. Licensee MDPI, Basel, Switzerland. This article is an open access article distributed under the terms and conditions of the Creative Commons Attribution (CC BY) license (https://creativecommons.org/licenses/by/4.0/).

## 1. Introduction

Land use and land cover (LULC) are fundamental factors shaping terrestrial environments. The expansion of urban, agricultural, and pasture lands has resulted in significant alterations to natural landscapes. These transformations exert a direct impact on water resources, influencing both streamflow and sediment transport [1]. Streamflow and sediment yield serve as pivotal components of the hydrological cycle, and changes in LULC

can modify river flow regimes [2]. The conversion of natural areas to agricultural uses can influence water availability; intensive irrigation practices, coupled with the removal of native vegetation, may diminish the recharge of subterranean aquifers and reduce baseflows in rivers [3].

Research focusing on the interaction between anthropogenic influences on landscape patterns and the effects of climate change on streamflow has attracted significant interest. However, much of the current literature has predominantly concentrated on the impacts of climate change and landscape pattern alterations separately [4,5]. While there have been numerous studies examining the link between climate change and streamflow, there is a conspicuous gap in applying this research to analyze land use and land cover trends in tropical basins, especially in Brazil [6]. In particular, the response of streamflow to changes in landscape patterns is an area that has yet to be thoroughly explored. This response varies across different basins and scenarios, a complexity arising from the fact that many previous studies have not adequately considered the nonlinear nature of hydrological streamflow regulation in relation to landscape pattern composition and configuration. Despite this gap, some studies have observed nonlinear responses, such as an increase in patch and edge density within cropland areas, leading to increased streamflow. Therefore, comprehending these complex relationships is crucial for effective water resource management and sustainable land use planning.

Despite their ecological and hydrological significance, the current trajectory of global warming, in conjunction with anthropogenic activities, has instigated substantial alterations in regional river runoff patterns since the early 20th century [7]. Changes in LULC have a direct bearing on local hydrology and sediment equilibrium within hydrological basins [8]. The study of LULC trends and their influences on streamflow and sediment yield plays a pivotal role in environmental preservation and in ensuring the availability of high-quality water for future generations. Research in this domain offers invaluable insights for policymakers, natural resource managers, and scientists, aiding in the promotion of sustainability and resilience of both aquatic and terrestrial ecosystems in the face of escalating environmental pressures [9]. In summary, this research on land–water dynamics in transforming climates and societies provides critical insights that can inform policy, enhance resource management, bolster resilience to climate change, and ultimately contribute to a more sustainable and equitable future. This study represents a departure from the conventional use of static data in hydrological modeling, thereby enhancing a critical aspect and significantly contributing to the field. Therefore, investigating the concurrent changes in LULC and their impacts on streamflow and sediment production serves as an essential procedure to assist decision makers in comprehending the ramifications of LULC changes on the water balance components.

Tropical humid forests, such as the Atlantic Forest biome, are terrestrial ecosystems characterized by immense biodiversity and structural complexity. They play significant roles in ecological functions such as regional climate regulation, water cycling, evapotranspiration, biodiversity maintenance, and greenhouse gas emission mitigation [10]. The hydrological regime of a basin is the product of complex interactions among climate, soil, topography, and LULC [11,12]. Any imbalance in these elements may cause alterations in hydrological processes, resulting in direct impacts on the environment, economy, and population of a region [13]. Among these, LULC is the most affected by human interventions [14,15].

Alterations in vegetative cover—such as converting forested areas to agricultural and pasture lands—are among the primary causes of water resource degradation [16]. In many coastal regions of Brazil, including the Pirapama River basin, expanding agricultural and grazing areas for sugarcane and cattle farming have led to significant landscape changes, primarily through the deforestation of the Atlantic Forest biome [2]. These changes induce soil erosion, pesticide leaching, and disruptions in terrestrial and aquatic ecosystems [14,15]. Currently, the Atlantic Forest is considered one of Brazil's most endangered biomes [16]. The forests in this biome are essential for maintaining river ecosystem integrity and ensuring water availability in reservoirs [17].

Though some studies have reported changes in streamflow behavior and sediment yield in basins near the coastline [18], quantitative analyses on the response of streamflow and sediment yield to LULC trends are still under-explored in the Atlantic Forest biome in Northeast Brazil [19]. This study distinguishes itself from other research on LULC changes by incorporating multi-year LULC data as a singular input in a simulation using the Soil and Water Assessment Tool (SWAT).

In Northeast Brazil, the Metropolitan Region of Recife (MRR) stands as one of the most populous and important regions, housing approximately 4,046,845 inhabitants [20]. The MRR faced severe water scarcity and rationing between 1998 and 2002. One solution was the construction of the Pirapama Reservoir in the Pirapama River basin. However, this basin has been experiencing considerable environmental degradation, largely due to the intensification of sugarcane farming activities [21].

Previous hydrological models, such as the Distributed Hydrological Model of Dams–AÇUMOD [22], Kinematic Runoff and Erosion Model–KINEROS [23], and Soil and Water Assessment Tool–SWAT [24], have been applied to analyze various hydrological processes in the Pirapama River basin [25–27]. Given the significant alterations in LULC coupled with climatic variability, a comprehensive understanding of their impact on local water resource management is crucial. Accordingly, this study investigates the effects of LULC changes on the dynamics of streamflow and sediment yield within a humid tropical basin of the Atlantic Forest biome in Brazil, with a focus on the period from 2000 to 2016.

## 2. Materials and Methods

### *2.1. Study Area*

The Pirapama River basin, encompassing an area of approximately 600 km$^2$, is situated between latitudes 8°07′29″ S and 8°21′00″ S and longitudes 34°56′20″ W and 35°23′13″ W (Figure 1). More precisely, it is located in the central-southern portion of the MRR. The Pirapama River extends over 80 km, originating at an altitude of 450 m in the municipality of Pombos in the Agreste region of Pernambuco State. This basin serves as one of the planning units for water resource management within the MRR [28]. Within this basin, the Pirapama, Gurjaú, and Sicupema reservoirs contribute significantly to the water supply for parts of the MRR.

According to the Köppen classification, the climate of the region is categorized as As′ (pseudotropical), characterized by hot and humid conditions. The average monthly temperature registers at 27 °C, and the mean relative humidity hovers around 70% [29]. The average annual precipitation within the basin is approximately 1500 mm, whereas the annual evaporation averages at 1200 mm [28]. Concerning precipitation regimes, the region exhibits two distinct periods: (a) dry, spanning from September to February, with monthly precipitation averages less than 60 mm, and (b) wet, from March to August [29].

LULC within the basin exhibits significant diversity, including urban and industrial development, agricultural estates, farms, rural settlements, minor hydroelectric facilities, sugarcane cultivation areas, the native Atlantic Forest, and mangroves [30]. Sugarcane cultivation remains the predominant agricultural activity, encroaching upon remaining forest patches and thereby compromising the environmental equilibrium of the area.

### *2.2. Land Use and Land Cover Dataset*

To assess the impact of LULC changes on streamflow and sediment yield, we employed historical data sets sourced from MapBiomas for 2000, 2004, 2007, 2010, 2013, and 2016. This specific timeframe was selected to align with the hydro-climatic data series used for model calibration and validation. Additionally, the initial two years (2000 and 2004) were chosen to mark the implementation and completion phases of the Pirapama Reservoir. The data were extracted from MapBiomas' Collection 2.3, which pertains to the Atlantic Forest, in GeoTiff format with LZW compression. These datasets were consolidated into a single file, wherein each band corresponds to one year within the adopted series (band 1 representing the first year). MapBiomas data sets are publicly available at MapBiomas

Database (http://mapbiomas.org/pages/database/mapbiomas_collection, accessed on 24 May 2023) [31,32].

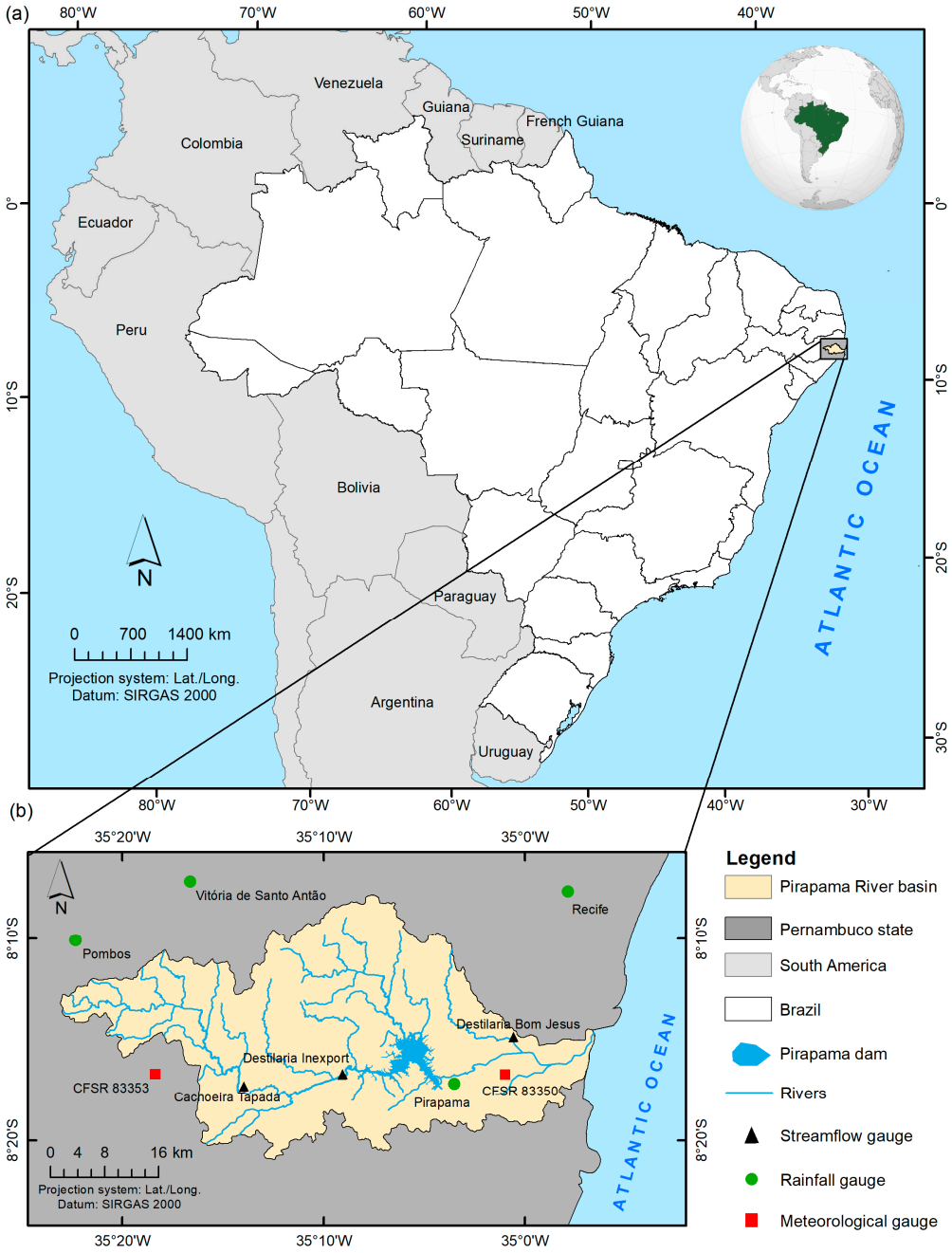


**Figure 1.** (**a**) Location of the Pirapama River basin in Brazil and in Pernambuco State, and (**b**) locations of rain, streamflow, and meteorological gauges used in the study.

The spatial datasets were generated through the pixel-to-pixel classification of Landsat satellite imagery, boasting a 30 m spatial resolution, using machine learning algorithms implemented on the Google Earth Engine platform. Recently, the MapBiomas Project has endeavored to automate the annual mapping of all Brazilian biomes through the use of Landsat imagery, achieving commendable outcomes [33]. For additional details on the methodology adopted for map composition, refer to the MapBiomas website (http://mapbiomas.org/pages/database, accessed on 15 May 2023).

### *2.3. Accuracy Assessment of LULC*

To validate the LULC classification generated by MapBiomas, we utilized imagery from Google Earth Pro spanning the period from 2005 to 2007. These images were selected based on optimal visibility conditions for target validation. The images facilitated the analysis of classification accuracy, and metrics for this analysis were computed using the Atacama plugin for QGIS (version 2.18). This plugin employs the stratified random sampling method for generating random points.

To quantitatively assess trends in LULC, the Kappa coefficient [34] was employed. The Kappa coefficient classification adopted in this study was delineated into six categories, each indicating the quality of the classified maps: poor ($\kappa < 0$), slight ($0 \leq \kappa < 0.2$), fair ($0.21 \leq \kappa < 0.4$), moderate ($0.41 \leq \kappa < 0.6$), substantial ($0.61 \leq \kappa < 0.8$), and very good ($0.81 \leq \kappa \leq 1$) [35].

The reliability of the LULC classification was further gauged through various metrics, including user's accuracy ($A_u$), producer's accuracy ($A_P$), overall accuracy ($GA$), and the Kappa coefficient ($\kappa$), as defined by the following equations:

$$\text{User's accuracy: } A_u = \frac{p_{ii}}{p_{i+}} \tag{1}$$

$$\text{Producer's accuracy: } A_p = \frac{p_{ii}}{p_{+i}} \tag{2}$$

$$\text{Overall accuracy: } GA = 100\frac{\sum_{i=1}^{m} p_{ii}}{n} \tag{3}$$

$$\text{Kappa coefficient: } \kappa = \frac{n\sum_{i=1}^{m} p_{ii} - \sum_{i=1}^{c} p_{i+}p_{+i}}{n^2 - \sum_{i=1}^{m} p_{i+}p_{+i}} \tag{4}$$

where $A_u$ and $A_P$ denote the user's and producer's accuracy, respectively, $GA$ represents overall accuracy, $\kappa$ is the Kappa coefficient, $p_{ii}$ is the proportion of area correctly classified for each category, and $p_{i+}$ and $p_{+i}$ are the marginal totals of the reference and classified data, respectively.

### *2.4. LULC Trend Analysis*

The non-parametric Mann–Kendall (MK) test [36,37], Pettitt [38], and Sen's slope estimator [39] were employed to scrutinize the time-series behavior of LULC in the Pirapama River basin. These statistical methods were selected to rigorously evaluate the spatiotemporal trends in land use and their corresponding runoff-erosion impacts.

### *2.5. Forest Fragmentation Analysis*

To assess forest fragmentation, we employed three ecological indices: Shannon-Weaver [40], Simpson [41], and Pielou [42]. The Shannon–Weaver index quantifies the diversity of fragment sizes within a forested landscape. A higher diversity of fragment sizes yields a higher index value. The Shannon–Weaver index is computed as follows:

$$S_W = \frac{\left[N\ln(n) - \sum_{i=1}^{E} n_i \ln(n_i)\right]}{N} \tag{5}$$

where $S_W$ represents the Shannon–Weaver index, $n_i$ is the number of sampled individuals within species $i$, $N$ is the total number of organisms across all species, and $E$ is the total number of species sampled.

The Simpson index evaluates the diversity of fragment sizes as well but assigns more weight to larger fragments. The index varies from 0 to 1, with higher values indicating less fragmentation. The Simpson index is calculated as:

$$S = \frac{\sum N(N-1)}{N_T(N_T-1)} \quad (6)$$

where $S$ represents the Simpson index, and $N_T$ is the number of organisms within species $i$.

The Pielou index assesses the evenness of fragment distribution within a landscape. A value approaching 1 signifies that the fragments exhibit regular shapes, while a value closer to 0 indicates irregular shapes. The Pielou index ($P$) ranges from 0 to 1, with higher values indicating greater levels of evenness in the community. A low $P$ value signifies that one or a few species dominate the community. At maximum evenness, $P$ = 1.

$$P = \frac{S_W}{\ln(N)} \quad (7)$$

To analyze the fragmentation of forested areas, the Forest Fragmentation Index ($F_f$) was calculated. A $F_f$ value close to 0 suggests that the forest remains relatively intact and unfragmented, while a value approaching 1 indicates high levels of fragmentation. In this study, four classes were identified: (a) high (value 1), (b) mild (value 0.6), (c) low (value 0.4), and (d) very low (value 0.2). The $F_f$ is computed using an equation that takes into account the total forest area ($T_f$), the area of the forest fragments ($A_f$), and the mean distance between them ($D_{mf}$). The index is calculated as follows:

$$F_f = \left(A_f \ / \ \mathrm{T}_f\right) \times (D_{\mathrm{mf}} \ / \ \mathrm{R}_{\mathrm{tf}}) \quad (8)$$

where $R_{tf}$ represents the ratio of total forest area to the overall land area.

### *2.6. Streamflow and Sediment Yield Simulation*

To analyze the response of streamflow and sediment yield, the SWAT model [43] was employed. This model is semi-conceptual, semi-distributed, physically based, and temporally continuous. The hydrologic balance in the SWAT is governed by Equation (9):

$$SW_t = SW_0 + \sum_{i=0}^{t} \left(P_d - Q_{\mathrm{sup}} - E_a - W_{\mathrm{vad}} - Q_{\mathrm{sub}}\right) \quad (9)$$

where $SW_t$ is the final soil water storage (mm), $SW_0$ is the initial soil water storage on day $i$ (mm), $t$ is time (days), $P_d$ is precipitation on day $i$ (mm), $Q_{\mathrm{sup}}$ is surface runoff on day $i$ (mm), $E_a$ is evapotranspiration on day $i$ (mm), $W_{\mathrm{vad}}$ is percolation on day $i$ (mm), and $Q_{\mathrm{sub}}$ is return flow (capillary rise from the vadose zone) on day $i$ (mm).

Sediment yield within the SWAT model is simulated using the Modified Universal Soil Loss Equation (MUSLE), given by Equation (10):

$$SYLD = 11.8(Q_{\mathrm{suf}} \times q_{\mathrm{peak}} \times area_{\mathrm{hru}})^{0.56} \times K_{\mathrm{USLE}} \times C_{\mathrm{USLE}} \times P_{\mathrm{USLE}} \times LS_{\mathrm{USLE}} \quad (10)$$

In this equation, $SYLD$ represents sediment yield in a given day (ton), $Q_{\mathrm{surf}}$ is the volume of surface runoff (mm), $q_{\mathrm{peak}}$ is the peak runoff flow rate ($m^3/s$), $area_{\mathrm{hru}}$ is the area of the hydrological response units (HRU) in hectares, $K_{\mathrm{USLE}}$ is the soil erodibility factor ($t{\cdot}h{\cdot}$ha/MJ/mm), $C_{\mathrm{USLE}}$ is the land management and cover factor (dimensionless), $P_{\mathrm{USLE}}$ is the conservation practices factor (dimensionless), and $LS_{\mathrm{USLE}}$ is the topographic factor (dimensionless).

The hydrological balance variables estimated using the SWAT model and scrutinized in this study include evapotranspiration ($ET$ in mm), surface runoff ($SURF_{\mathrm{Q}}$ in mm), infiltration ($GW_{\mathrm{Q}}$ in mm), and sediment yield ($SYLD$ in ton/ha). For more detailed information about the SWAT model, please refer to the studies of Arnold et al. [24,43].

The SWAT is ubiquitously utilized in hydrological research, specifically for quantifying the impacts of climatic and land use transformations on both the hydrological cycle and water quality metrics. One of SWAT's distinguishing features is its robust capability to incorporate agricultural management practices—including irrigation, fertilizer and pesti-

cide application, and tillage operations—into its simulations. This renders it particularly efficacious for studies centered on catchments with substantial agricultural activity. Given its wide-ranging applicability across diverse geographic locales, the SWAT is optimally suited for evaluating the repercussions of LULC alterations within the basin under study.

It is crucial to differentiate this research from prior SWAT investigations that predominantly employed static land cover data to scrutinize hydrological outcomes. This work accentuates the indispensable role of dynamic LULC data in mitigating the propensity for over-parameterization during model calibration, a common pitfall when utilizing static LULC datasets. The incorporation of dynamic LULC data affords a temporally nuanced representation of the catchment's evolving land cover dynamics, thereby enhancing model fidelity.

Unique to this study is its methodology of integrating multi-year LULC data into a single SWAT simulation. This distinct approach differentiates it from numerous other research efforts focused on the hydrological consequences of LULC changes, thereby offering a fresh perspective to the scientific discussion on this topic. It is important to note that while there are springs in the study area, these were not subjected to more in-depth analysis in this particular study.

#### 2.6.1. SWAT Input Database

To perform initial watershed modeling, the SWAT requires three distinct geospatial files: a digital elevation model (DEM), soil types, and LULC. The study area was divided into 29 sub-basins based on a 30 m spatial resolution DEM, sourced from the United States Geological Survey (USGS). These data were accessed at http://earthexplorer.usgs.gov (accessed on 15 April 2023) (Figure 2a).

The baseline LULC map utilized was constructed based on two satellite images from the Landsat 5/TM sensor, dated 6 June 2005 and 28 July 2007, each with a spatial resolution of 30 m (orbit 214/point 066). These data were downloaded on 13 January 2023, and the images were obtained from http://earthexplorer.usgs.gov, accessed on 30 January 2023. These specific images were selected due to their minimal cloud cover, which facilitated the validation of land use classification for use as a reference map. In this study, supervised classification utilizing the maximum likelihood method in ArcGIS 10.2 was employed to classify the LULC into the following categories: water, urban area, bare soil, dense vegetation, shrubland, and sugarcane (Figure 2b).

The basin was partitioned into 1641 hydrological response units (HRUs), which are homogeneous areas exhibiting uniform soil types, land use, and slope. In this study, five slope classes were delineated (0–3%, 3–8%, 8–20%, 20–45%, and >45%). Soil types, mapped at a 1:100,000 scale (Figure 2c), were sourced from the EMBRAPA Soils portal on 15 December 2022, available at http://www.sisolos.cnptia.embrapa.br. These data were downloaded on 10 February 2023. Figure 3 outlines the methodological steps adopted for the development of this research.

#### 2.6.2. Meteorological Data

For the completion of this study, a diversified range of meteorological data was utilized to scrutinize the variability in streamflow and sediment yield. In this investigation, meteorological variables such as solar radiation, relative humidity, wind speed, and minimum and maximum temperatures were acquired from two grid datasets derived from the Climate Forecast System Reanalysis (CFSR) for the period from 1997 to 2010, available at https://globalweather.tamu.edu and accessed on 15 December 2022. Additionally, daily rainfall data spanning the years 2000 to 2010 were obtained on 15 December 2022 from https://www.apac.pe.gov.br [44]. Concurrently, monthly streamflow data from a trio of stations located within the study's geographical boundaries were sourced on 15 December 2022 from https://www.snirh.gov.br/hidroweb [45]. Table 1 shows the details of the gauge stations employed in the study.

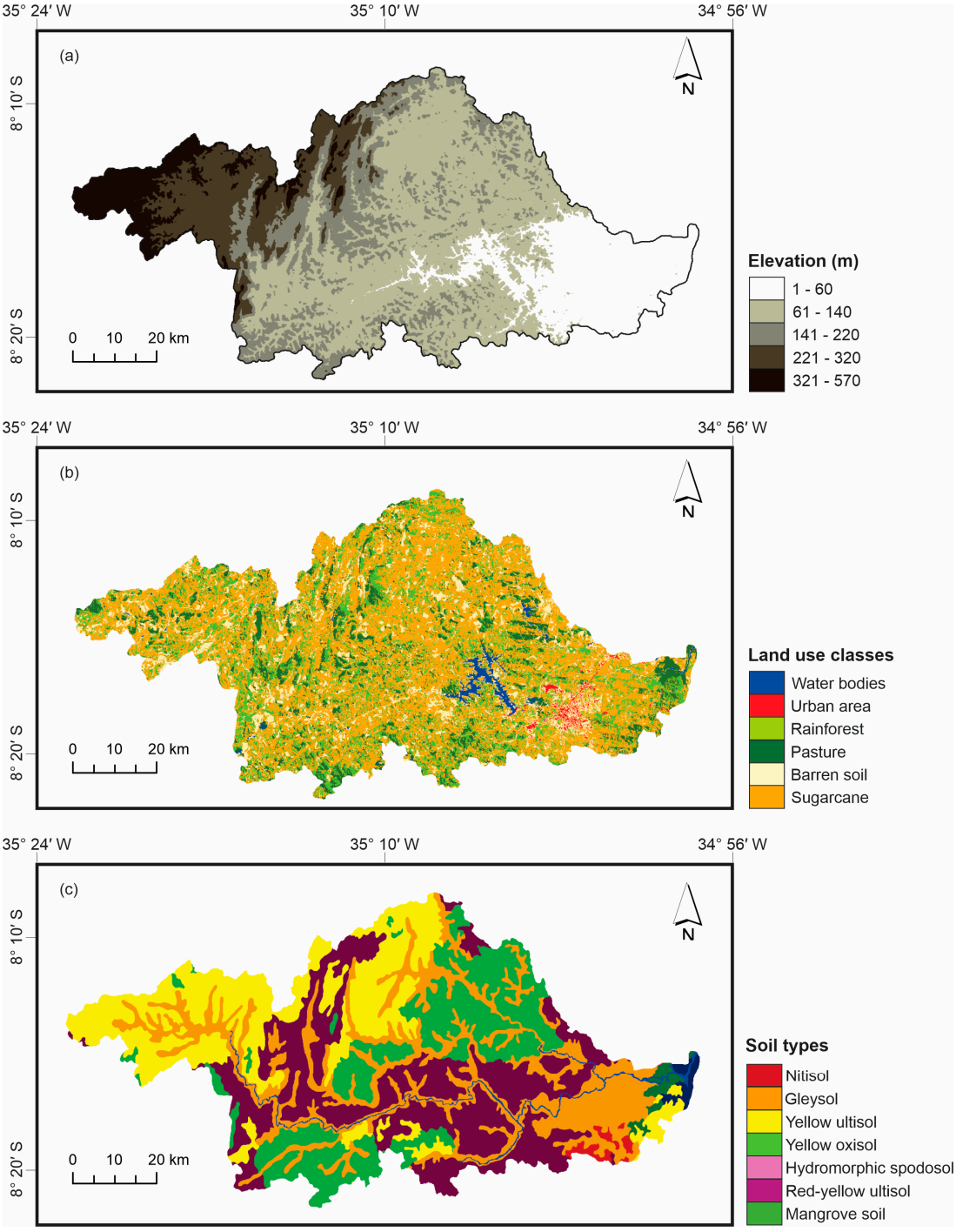


**Figure 2.** (**a**) Digital elevation model, (**b**) land use and land cover, and (**c**) soil types of the Pirapama River basin.

To ensure data compatibility and homogeneity, the chosen period was congruent with the flow series employed for hydrological modeling, specifically spanning the years 2000 to 2010. Monthly temperature data from a single station covering the identical temporal window were obtained from the National Institute of Meteorology [46]. The data from these stations underwent a meticulous quality control process to assess the reliability and consistency of the values used. Table 1 delineates the geographical coordinates and temporal span of the gauge stations utilized in this study, thereby providing a comprehensive overview of data provenance.

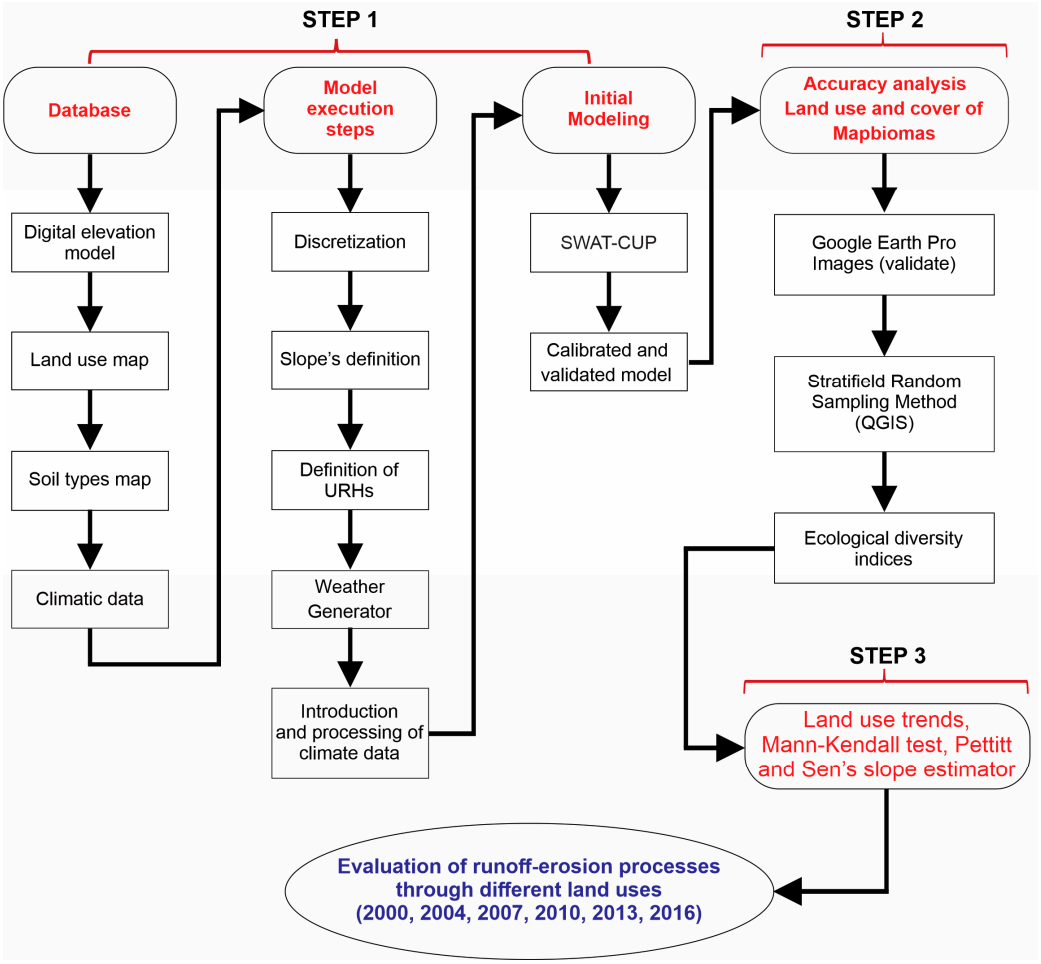


**Figure 3.** Flowchart depicting the methodological steps undertaken.

**Table 1.** Characteristics of gauge stations employed in the study.

| Name | Type | Data Period | Longitude | Latitude |
|---|---|---|---|---|
| Pirapama | Rainfall | 1987–2010 | −35°03′50″ | −8°16′43″ |
| Vitória de Santo Antão | Rainfall | 1920–2010 | −35°16′37″ | −8°13′32″ |
| Pombos | Rainfall | 2000–2010 | −35°25′30″ | −8°08′18″ |
| Recife | Rainfall | 1987–2010 | −34°43′10″ | −8°05′25″ |
| 83353 CFSR grid | Meteorological | 2000–2010 | −35°20′00″ | −8°25′00″ |
| 83350 CFSR grid | Meteorological | 2000–2010 | −35°00′00″ | −8°25′00″ |
| Cachoeira Tapada | Streamflow | 1986–2010 | −35°15′57″ | −8°15′59″ |
| Destilaria Inexport | Streamflow | 2000–2010 | −35°09′24″ | −8°16′55″ |
| Destilaria Bom Jesus | Streamflow | 2000–2010 | −35.00′47″ | −8°15′52″ |

#### 2.6.3. Calibration and Validation of the SWAT Model

The modeling process was divided into three phases: warm-up (1997–1999), calibration (2000–2006), and validation (2007–2010). The SWAT model underwent validation, specifically tailored for its application in the Pirapama River basin, using the split-sample test. To analyze the sensitivity and uncertainties of the parameters, as well as the calibration and validation between observed and simulated data in the SWAT model, we utilized the SWAT-CUP (Calibration Uncertainty Program) software package [47], deploying the SUFI-2 algorithm through a 500-simulation iteration [48]. The SUFI-2 algorithm uses the Latin hypercube sampling method to define the parameters, commencing with a user-defined range of values. To analyze the sensitivity of the parameters in the modeling, we used the P-factor and R-factor metrics [47], which assess the reliability of the fit and the degree of

efficiency of the calibrated model. It is noteworthy that the basin lacks sediment-related data. Following the model validation, we simulated the streamflow and sediment yield under varying land use and land cover scenarios.

#### 2.6.4. Performance Indices of Hydrologic Modeling

To assess the congruence between observed and estimated flow values during both the calibration and validation phases, two statistical indices were employed: (a) the Nash–Sutcliffe efficiency coefficient (*NSE*) and (b) Pearson's determination coefficient ($R^2$) [49,50]. The NSE quantifies the relative accuracy of the simulated data compared to the observed data and ranges from negative infinity to 1. A value of $NSE = 1$ implies a perfect fit between the observed and simulated datasets. The formula for computing the NSE is expressed as:

$$\mathrm{NSE} = 1 - \frac{\sum_{i=1}^{n} [(Q_{obs,i}) - (Q_{sim,i})]^2}{\sum_{i=1}^{n} \left[Q_{obs,i} - \overline{Q_{obs}}\right]^2} \quad (11)$$

where $Q_{obs}$ represents the observed event, $Q_{sim}$ denotes the event as simulated by the model, $\overline{Q_{obs}}$ is the mean value of the observed events during the simulation period, and $n$ is the total number of events.

Pearson's determination coefficient ($R^2$) evaluates the linear association between the observed and simulated variables. This coefficient also ranges from negative infinity to 1, with 1 indicating perfect association. The coefficient is derived using the following equation:

$$R^2 = 1 - \frac{\sum_{i=1}^{n} (Q_{obs,i} - Q_{sim,i})^2}{\sum_{i=1}^{n} \left(Q_{obs,i} - \overline{Q_{obs}}\right)^2} \quad (12)$$

### *2.7. Evaluation of Streamflow and Sediment Yield*

To assess potential variations in the runoff-erosion processes in the Pirapama River basin, we utilized LULC scenarios from the years 2000, 2004, 2007, 2010, 2013, and 2016. Each land-use type was employed to simulate hydro-sedimentological dynamics, substituting these different scenarios into the SWAT for each new iteration while maintaining consistent climatic data, soil types, and slope. Based on these varying scenarios, six sets of flow and sediment yield simulations were produced. The analyses and comparisons between the scenarios were conducted with reference to key components of the hydro-sedimentological balance, including flow rate, evapotranspiration, percolation, sediment yield, and seasonal flow rate averages. For these variables, the basin-wide average was computed for each component.

## 3. Results

### *3.1. LULC Change Analysis*

Table 2 delineates the confusion matrix, user accuracy, and producer accuracy acquired subsequent to the validation of samples chosen for the 2007 MapBiomas map. The producer accuracy was determined to be 0.88, while user accuracy oscillated between 0.80 and 1.00. In the matrix, rows represent information from the reference map, while columns pertain to the map under validation. The diagonal elements indicate the precision of each land-use class, while off-diagonal values correspond to the commission and omission errors for each class.

According to the confusion matrix assessment, most classes demonstrated high accuracy or precision in classification, exceeding 70% accuracy. However, classes corresponding to scrubland, urban area, and sugarcane manifested a higher proportion of misclassified samples—that is, those with a higher number of pixels assigned to incorrect categories or land-use classes (producer accuracy and omission error). In the producer category, the classes of water, dense vegetation, and mangrove exhibited elevated accuracies compared

to other classes, registering respective correctness percentages of 0.94, 0.96, and 1.00. Both producer and user accuracies suggest that the results range from good to excellent. Moreover, the land cover classifications showed good agreement with each annual classified map, corroborated by a Kappa index of 0.85. The overall precision of the land-use classes was 88% (0.88), which is considered excellent (Table 2). Generally, although classifications did not achieve 100% accuracy for all land-use classes, both in terms of producer and user hits, the results were deemed satisfactory, as each category registered accuracies above 60% relative to the correctly classified pixels of the total samples collected for each use. Table 3 presents the temporal shifts in land use from 2000 to 2016. The data indicate an increase in the classes of urban area, pasture, water, and sugarcane, juxtaposed with a decline in the mangrove and rainforest regions.

**Table 2.** Confusion matrix, producer, and user accuracy for MapBiomas.

| Classes | Water | Urban Area | Rainforest | Pasture | Mangrove | Sugarcane | Total | User Accuracy |
|---|---|---|---|---|---|---|---|---|
| Water | 15 | 0 | 0 | 0 | 0 | 0 | 15 | 1.00 |
| Urban area | 0 | 15 | 0 | 0 | 0 | 0 | 15 | 1.00 |
| Rainforest | 0 | 0 | 27 | 2 | 0 | 1 | 30 | 0.90 |
| Pasture | 0 | 0 | 0 | 28 | 0 | 2 | 30 | 0.93 |
| Mangrove | 1 | 1 | 1 | 3 | 24 | 0 | 30 | 0.80 |
| Sugarcane | 0 | 2 | 0 | 7 | 0 | 41 | 50 | 0.82 |
| Total | 16 | 18 | 28 | 40 | 24 | 44 | 170 | – |
| Producer accuracy | 0.94 | 0.83 | 0.96 | 0.70 | 1.00 | 0.93 | – | 0.88 |

**Table 3.** Land-use classes in the basin from 2000 to 2016.

| Classes | Dense Vegetation ($km^2$) | Mangrove ($km^2$) | Pasture ($km^2$) | Sugar Cane ($km^2$) | Urban Area ($km^2$) | Water ($km^2$) |
|---|---|---|---|---|---|---|
| 2000 | 212.11 | 3.59 | 34.50 | 323.65 | 4.58 | 1.39 |
| 2004 | 184.75 | 3.44 | 32.56 | 347.71 | 5.28 | 6.08 |
| 2007 | 191.87 | 4.32 | 19.22 | 351.58 | 6.15 | 6.68 |
| 2010 | 204.47 | 3.15 | 38.70 | 320.35 | 7.23 | 5.92 |
| 2013 | 187.62 | 2.81 | 81.67 | 294.57 | 7.99 | 5.16 |
| 2016 | 160.59 | 2.69 | 44.84 | 360.95 | 8.45 | 2.30 |
| **Variation (%)** | −24.29 | −25.07 | 29.97 | 11.52 | 84.50 | 65.47 |

The statistical analysis of forest fragmentation was conducted using diversity metrics such as the Shannon–Weaver index (1.041), Simpson index (0.535), and Pielou index (0.528). These metrics reveal various facets of species richness and evenness in the forest cover within the Pirapama River basin, thereby illuminating the ecosystem's complex biodiversity. Figure 4 delineates the temporal evolution of forest cover from 2000 to 2016. It depicts (a) the initial state of forest cover, (b) the status as of 2016, (c) areas of land use and land cover (LULC) change between 2000 and 2016, and (d) the spatial distribution of the Forest Fragmentation Index across the Pirapama River basin.

Notably, there is a discernible decline in the area covered by forest within the basin during the study period, as shown in Figure 4a,b. This loss of forest cover has consequential impacts on hydrological processes, such as reducing rainfall interception, increasing surface runoff, and diminishing aquifer recharge rates. Additionally, the absence of vegetation exacerbates soil erosion and degradation, adversely affecting the quality and availability of water resources.

Figure 4c discloses that a substantial portion of the basin underwent changes in LULC over the analyzed period. Intriguingly, the eastern part of the basin has largely retained its original configuration, while the remaining areas have experienced transformations. These findings are consistent with Figure 4d, which displays the calculated Forest Fragmentation

Index for the study area, with values ranging from 1 to 8. It is important to emphasize that categories 6 and 8 registered the largest extent of fragmentation.

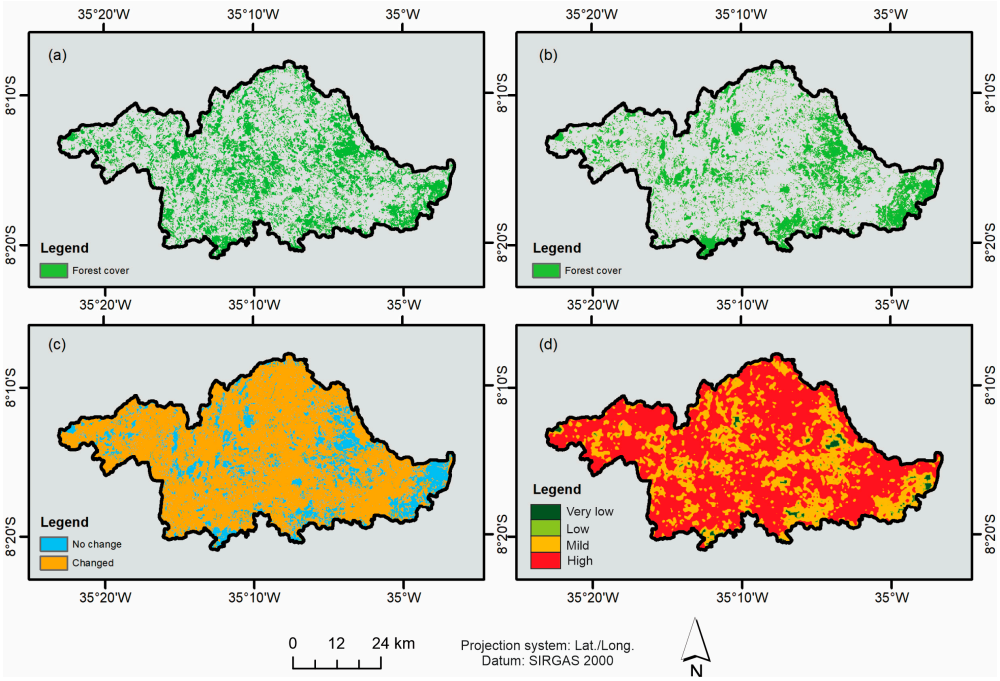


**Figure 4.** (**a**) Forest cover in 2000, (**b**) forest cover in 2016, (**c**) areas with and without LULC changes, and (**d**) spatial distribution of the Forest Fragmentation Index for the Pirapama River basin.

### *3.2. Trends in LULC Evolution*

Figure 5 depicts the LULC trends in the Pirapama River basin for the years under scrutiny. The findings reveal both increasing and decreasing trends in LULC during the examined period. The associated statistical significances based on non-parametric tests are presented in Table 4. For all land-use classes, the Mann–Kendall test p-values demonstrated a 5% level of significance. Consequently, the null hypothesis of no trend was rejected, identifying a decreasing trend. Thus, the time series of the analyzed land-use classes cannot be considered stationary.

Significant downward trends were observed in the mangrove and rainforest classes, indicating a notable loss of vegetation cover over the years examined. Conversely, the urban area and water classes exhibited a statistically significant ($p$-value < 0.05) upward trend. Overall, the basin experienced a net loss of natural vegetation over the examined period, corroborated by [51]. Other classes, including sugarcane, pasture, and water, did not exhibit statistically significant trends in either increase or decrease. The breakpoint years indicated by the Pettitt test for the mangrove and urban area classes were 2009 and 2008, respectively.

### *3.3. Analysis of Streamflow for Different LULC Scenarios*

Streamflow simulations were conducted for the six soil cover scenarios previously described. Figure 6a,b present the simulated streamflow results for various land uses, including the calibrated period (baseline), as well as the mean monthly precipitation. In Figure 6a,b, it is evident that the simulated streamflow for all analyzed land use scenarios in the Pirapama River basin displays a rapid temporal response to regional rainfall events, with a slight decrease in streamflow for the 2000 and 2013 scenarios, particularly between the months of January and May. Scenarios corresponding to 2004, 2007, 2010, and 2016 exhibited estimates more akin to the baseline. These results indicate a minimal alteration in the variability of simulated streamflows among the different scenarios, except for estimates obtained for the years 2000, 2013, and 2016, which were markedly discrepant. Concerning

land use during these periods, there was solely a decline in dense and low vegetation in 2016, relative to other years, accompanied by an increase in sugarcane and urban areas (Table 5).

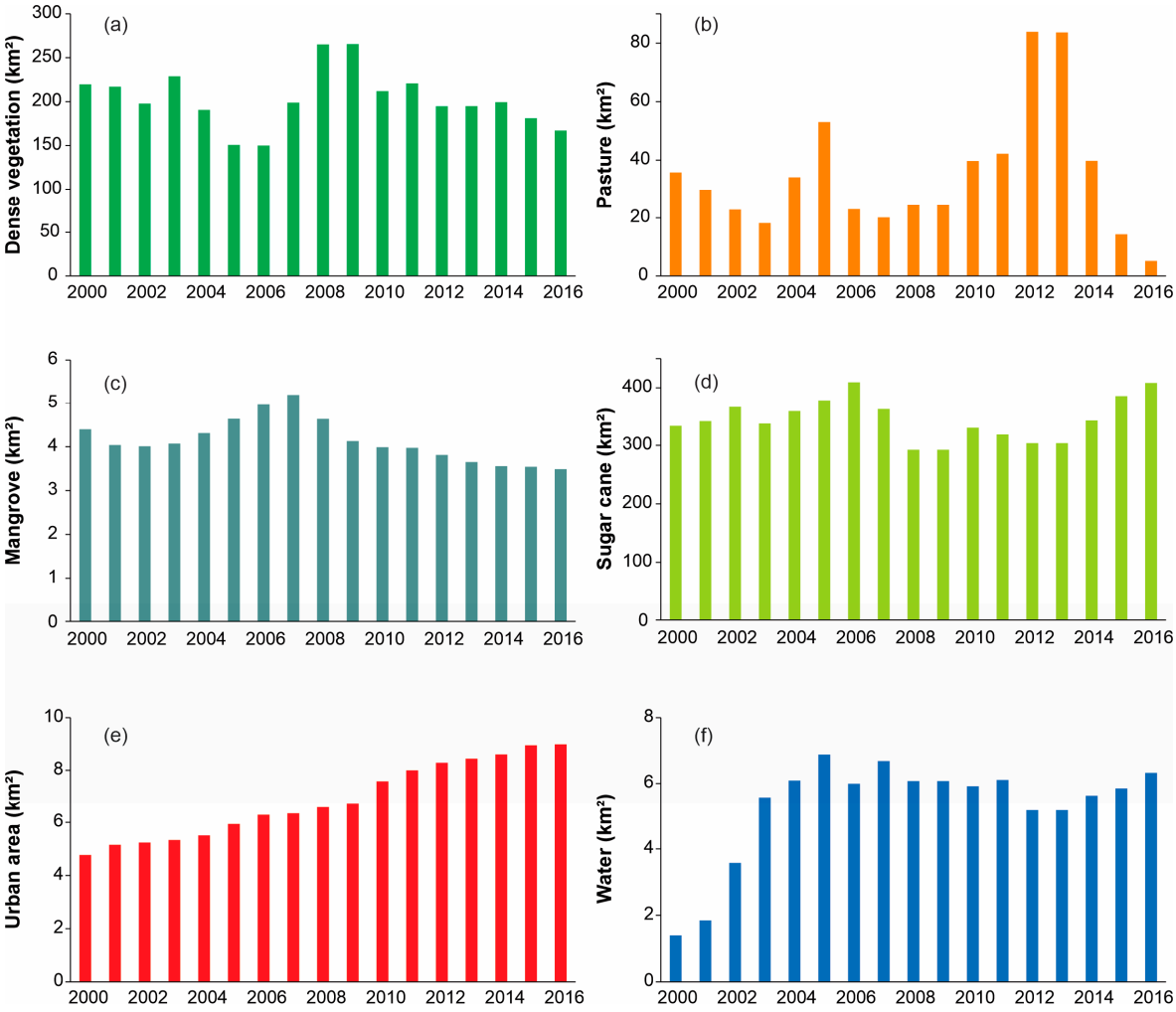


**Figure 5.** Trends for each LULC in the Pirapama River basin between 2000 and 2016: (**a**) dense vegetation, (**b**) pasture, (**c**) mangrove, (**d**) sugar cane, (**e**) urban area, and (**f**) water.

**Table 4.** Results of MK, Pettitt, and Sen tests for land use and land cover series.

| Land Use and Cover | Mann–Kendall | | | | Pettitt | | | Sen's Slope ($\alpha$ = 95%) |
|---|---|---|---|---|---|---|---|---|
| | z | *p*-Value | S | Tau | U | *p*-Value | Year of Change | |
| Rainforest | −0.765 | $4.40 \times 10^{-1}$ | −18 | −0.15 | 25 | $8.45 \times 10^{-1}$ | 2011 | −132.47 |
| Pasture | 0.495 | $6.20 \times 10^{-1}$ | 12 | 0.1 | 55 | $6.79 \times 10^{-1}$ | 2014 | 55.16 |
| Mangrove | −2.927 | 0.00 | −66 | −0.55 | 63 | $8.41 \times 10^{-3}$ | 2009 | −6.54 |
| Sugarcane | 0 | 1.00 | 0 | 0 | 35 | $3.70 \times 10^{-1}$ | 2007 | −2.87 |
| Urban area | 5.357 | 0.00 | 120 | 1 | 64 | $7.06 \times 10^{-3}$ | 2008 | 28.59 |
| Water | 0.451 | $6.50 \times 10^{-1}$ | 11 | 0.092 | 35 | $3.70 \times 10^{-1}$ | 2003 | 2.16 |

In summary, the variations observed in the simulated streamflows across the examined scenarios indicate a modest trend of increasing streamflows. This suggests that land use and land cover alterations within the basin have been sufficiently substantial to directly impact streamflow dynamics, as corroborated by the data presented in Table 5.

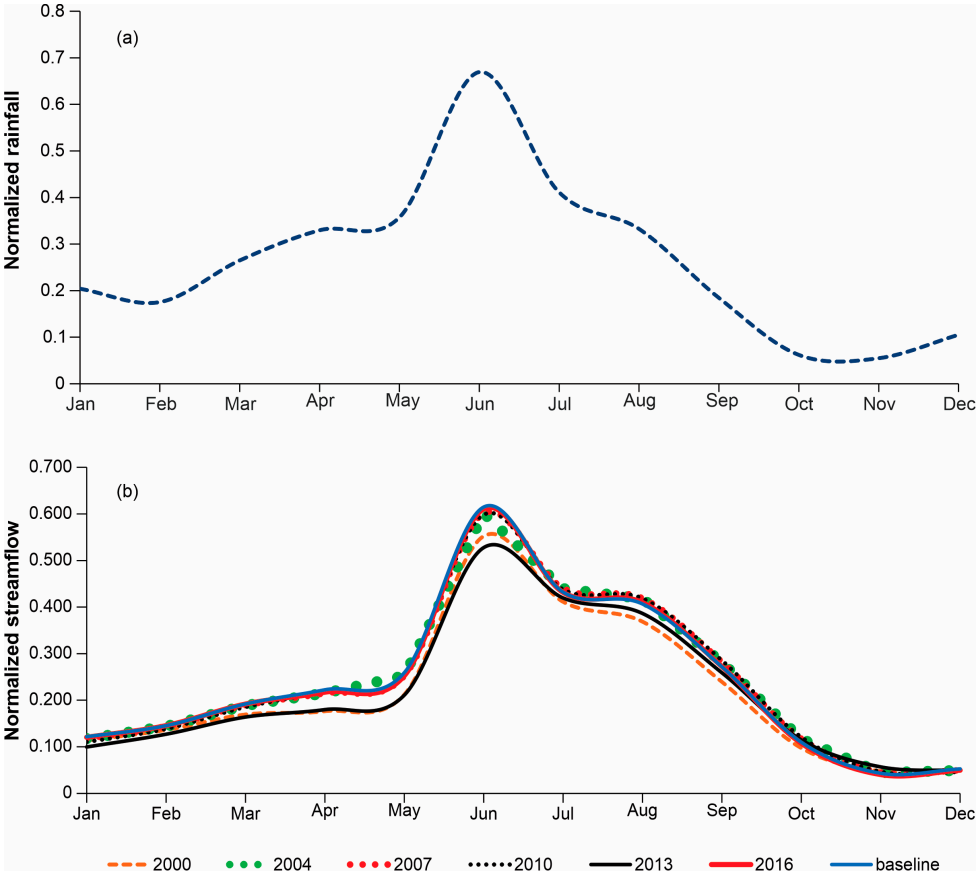


**Figure 6.** (**a**) Mean monthly normalized precipitation and (**b**) mean monthly simulated normalized streamflow for various LULC scenarios.

**Table 5.** Estimates of hydrological balance variables and sediment yield for estimated scenarios and the baseline.

| LULC | *ET* (mm) | $SURF_Q$ (mm) | $GW_Q$ (mm) | *SYLD* (ton/ha) |
|---|---|---|---|---|
| Land use 2000 | 679.10 | 381.23 | 639.79 | 12.00 |
| Land use 2004 | 688.40 | 387.58 | 626.03 | 9.63 |
| Land use 2007 | 689.80 | 386.94 | 625.00 | 8.90 |
| Land use 2010 | 688.80 | 377.40 | 631.82 | 10.10 |
| Land use 2013 | 686.40 | 376.57 | 633.41 | 20.42 |
| Land use 2016 | 689.10 | 398.87 | 611.20 | 4.83 |
| Baseline | 670.7 | 340.6 | 681.47 | 6.47 |

### *3.4. Hydrological Balance Analysis for Different LULC Scenarios*

The results presented herein take into account variables such as surface runoff (*SURF*), deep aquifer percolation (*GW*), actual evapotranspiration (*ET*), and sediment yield (*SYLD*). The analysis suggests that variations in land use across the examined scenarios are not markedly distinct; consequently, the hydrological balance estimations exhibit minor differences in surface runoff, percolation, and especially in evapotranspiration from one scenario to another (Figure 7 and Table 5).

Comparing these land use outcomes with the baseline data from 2007 reveals minor percentage differences despite more significant variations in dense and sparse vegetation between the baseline and other land use plans. The percentage differences demonstrate that land uses from 2000 to 2016 manifest higher values of evapotranspiration and surface runoff relative to the baseline and lower values of percolation, with differences reaching up to −10.31%.

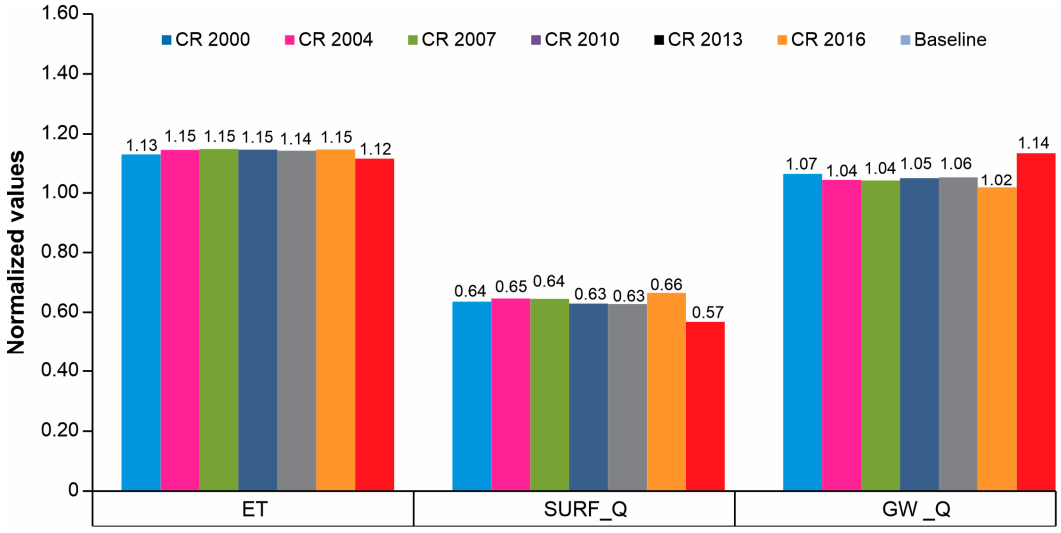


**Figure 7.** Annual average of the water balance in the Pirapama River basin and the percentage difference in relation to different land uses and the baseline.

With respect to the surface runoff estimates for each sub-basin in the real scenarios analyzed (Figure 8), a consistent pattern emerges across the scenarios for both higher and lower estimates. However, specific variations within each sub-basin in individual scenarios are evident, with elevated runoff rates observed in sub-basins 1, 6, 7, 10, 13, 15, 18, 21, 23, 26, and 29, where estimates range from 558 to 667 mm. The highest rates of sub-basin runoff were found in the 2004, 2007, and 2010 scenarios, aligning with the observed flow patterns.

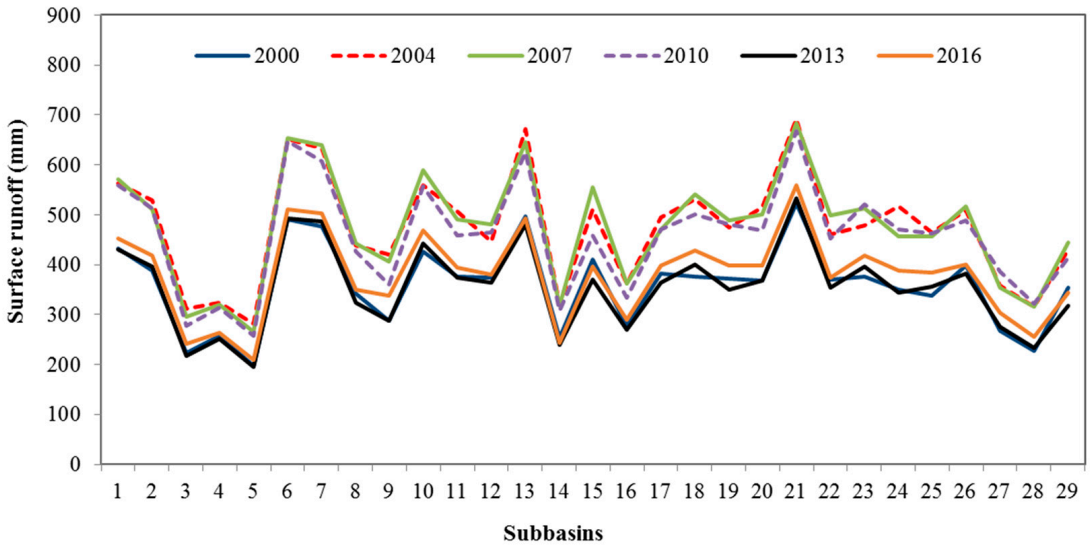


**Figure 8.** Estimate of surface runoff (mm) per sub-basin for different soil uses.

Through these analyses, it is understood that the changes in land use within the real scenarios studied did not directly and perceptibly influence the hydrology of the basin for this region. However, it is known that abrupt and significant changes in land use and occupation within basin areas can compromise the hydrologic dynamics of these regions. The authors of [52] worked with hypothetical land-use scenarios (S = Scenarios), converting forest to pasture (20%–S1 and 50%–S2, respectively) and pasture to forest (20%–S3 and 50%–S4, respectively). They observed increases in total runoff, peak flow, and decreases in baseflow and evapotranspiration for scenarios S1 and S2 and the opposite for reforestation scenarios (S3 and S4). Consequently, they suggested that significant changes in land use

can generate both positive impacts, such as reduced surface runoff and increased baseflow, and negative impacts, such as increased soil erosion and flood risks. According to [53], accelerated changes in land use can have consequences for regional hydrology and the hydroelectric potential of power plants. In this context, the authors evaluated four scenarios of land use and cover change in the Tocantins–Araguaia River basin (TAW), focusing on the Tucuruí Hydroelectric Plant (THP) downstream of the TAW. They found that forested areas were replaced by pastures, followed by sugarcane, then reforestation vegetation, and finally, by regenerated forest. The results indicated a decrease in the annual evapotranspiration rate and an increase in surface runoff and flow, but without an increase in energy produced at the THP due to the turbines' lag in converting excess water into energy, resulting in energy production losses.

Thus, it is understood that the hydrologic cycle is closely linked to land use and occupation, so accelerated changes in land cover have been considered one of the most influential factors affecting the availability of freshwater [54]. The global scientific community has overwhelmingly demonstrated that changes in land use can interfere with the dynamics of the water balance, causing both positive and negative impacts on society [55–60].

Regarding sediment yield, the simulations indicated greater variations, resulting in higher percentage differences, especially for CR2013 (215.61%), which had the largest difference compared to the baseline among the scenarios (Figure 9 and Table 5). When compared with the variability of land uses, a behavior more aligned with low-lying vegetation was observed, indicating that as this class varies across the scenarios, so does sediment yield (Figure 9). This may be attributed to the influence that the class labeled "pasture" (PAST) in the SWAT model, designated as low-lying vegetation in this research, has on sediment yield behavior and how alterations to this use over the years affect the dynamics of this estimate. According to research [61] in the Cobres River basin, located in the semi-arid region of Portugal, the authors found that Scenario 2 (pasture) produced the highest sedimentation rate among the scenarios, whereas Scenario 3 (forest) presented the lowest average value. The authors concluded that land-use types interfere with hydro-sedimentological processes and, consequently, with flow regimes and sediment yield in watersheds, particularly those where flow is ephemeral.

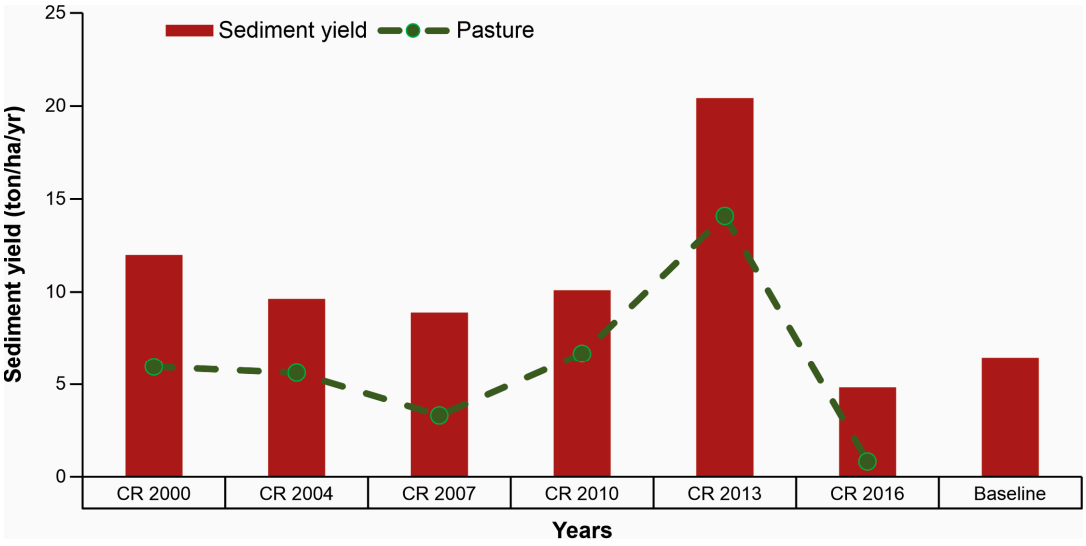


**Figure 9.** Annual average sediment yield in the Pirapama River basin and the percentage difference compared to the baseline scenario.

The spatial distribution of sediment yield estimates by sub-basins generally indicates areas in the western part of the basin as having higher sediment yield rates, ranging between 18 and 59 ton/ha in the scenarios from 2000 to 2013 (Figure 10). Most of these areas are characterized by elevated topography, a factor contributing to the increased rates.

Furthermore, these areas predominantly consist of Acrisols soils, which are more prone to erosion. The 2016 scenario exhibited lower sediment yield rates (0–18 ton/ha), possibly influenced by a greater prevalence of dense vegetation and sugarcane and less pasture compared to other scenarios.

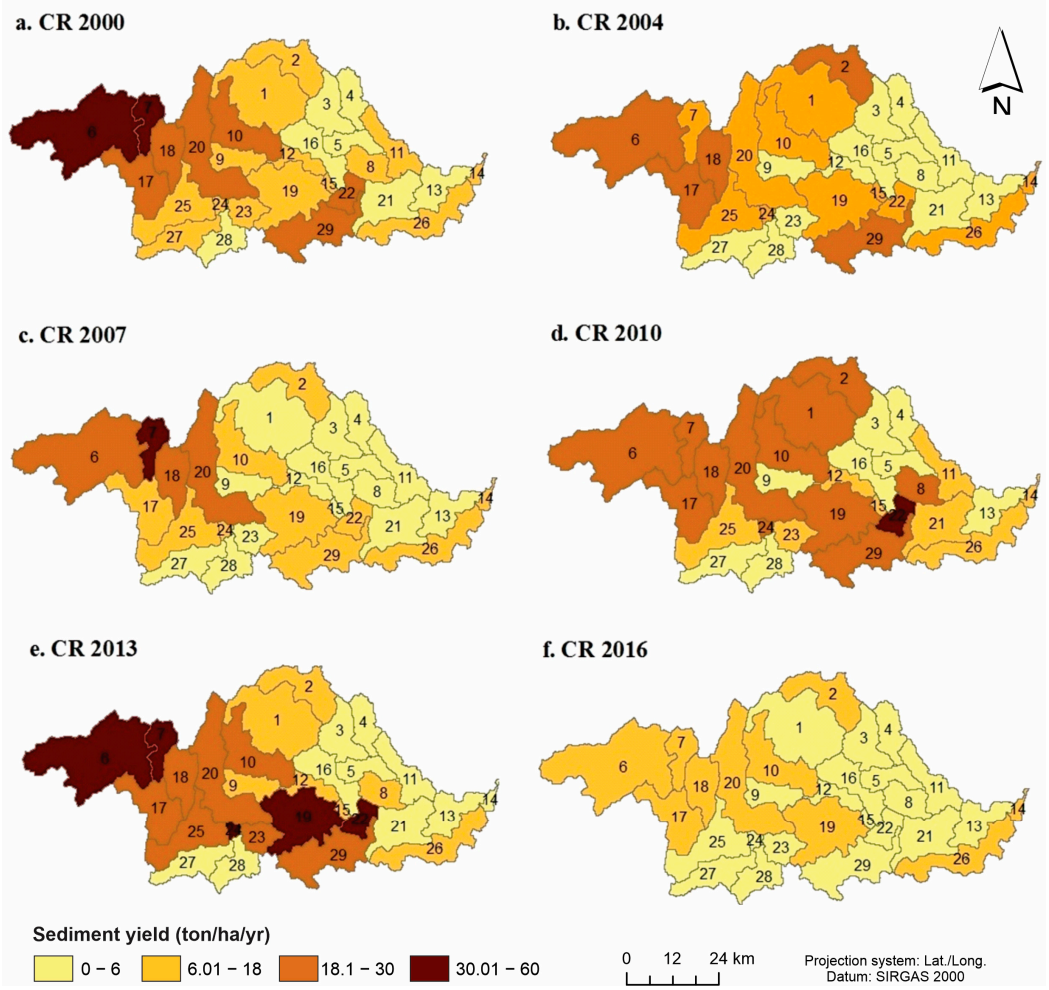


**Figure 10.** Spatialization of sediment yield estimates by sub-basin for the analyzed scenarios in the Pirapama River basin.

In sub-basins 15, 16, 19, and 22, where the Pirapama reservoir is located, elevated sediment yield rates are particularly observed from 2004 onward, especially for the 2010 and 2013 scenarios (Figure 10). According to [62], these areas possess physical and geomorphological features predisposed to erosion that could affect the reservoir's water volume when eroded material accumulates at the lake bed.

Elaborating further on the subject of land use, many of these areas have a higher prevalence of sugarcane and low-lying vegetation—factors that exacerbate erosion. In the case of sugarcane cultivation, present across much of the basin, soil erosion and sediment transport to lower areas of the basin are more likely to occur during periods of harvest when the soil is exposed. However, when sugarcane cultivation is combined with mulch (residue from the crop itself), soil and water losses are minimized [63]. In this practice, mowed grass (dry grass, straw, and crop residue) and plant remnants are maintained on the soil surface between the planted rows. This assists in protecting the soil from rain impact, maintaining soil moisture, controlling soil temperature, preserving beneficial microorganisms, and promoting water infiltration while also reducing runoff speed, thereby diminishing erosion losses [64]. According to [65], the absence of forest-type vegetation results in increased

sediment yield as precipitation intensifies, whereas the presence of such vegetation reduces the quantity of sediment produced under the same precipitation conditions.

Ref. [66] determined in their study of a watershed within the Caatinga biome in the state of Paraíba that the most substantial land use change occurred following the removal of natural vegetation for the utilization of areas of exposed soil, typified by livestock farming in the region and other activities. This shift significantly impacted the hydro-sedimentological process estimates, revealing a substantial increase in surface runoff (137%) and sediment yield (290%) across the various scenarios employed. However, it is crucial to emphasize that other variables—such as rainfall distribution throughout the year, soil depth, and terrain slope—are also integral to the analysis of land use and cover changes and their impact on hydro-sedimentological dynamics.

## 4. Discussion

### *4.1. Limitations, Advantages, and Applications of the Study*

Long-term hydrological response simulations in basins are often conducted under the assumption of static LULC conditions. However, this assumption is not a realistic representation, particularly in basins subject to frequent anthropogenic alterations, such as the Pirapama basin, which has experienced significant shifts in LULC. This research analyzed both LULC trends and hydrological balance component behavior using the SWAT model, providing a more realistic simulation of the Pirapama River basin's hydrology. A notable advantage of this study over prior LULC change investigations is the incorporation of dynamic LULC input under various scenarios into the SWAT model. This approach enabled efficient modeling that captured the temporal continuity of hydrological processes affected by historical LULC changes. Therefore, the methodology adopted herein facilitates a robust and accurate hydrological assessment, contributing significantly to our understanding of how LULC changes impact key hydrological balance components.

The uncertainties in the SWAT model were based on the sensitivity analysis of the most sensitive parameters. This sensitivity analysis revealed that parameters related to the LULC Soil Conservation Service Curve Number method (CN2) [67] and the Universal Soil Loss Equation C-factor (USLE C-factor) [68] were the main factors influencing the modeling. These parameters are crucial in assessing soil erosion susceptibility across various land use categories. The USLE C-factor, reflecting land cover and management practices, significantly impacts soil erosion rates. Meanwhile, CN2 is vital for understanding the erosive potential associated with specific land uses. Analyzing the interplay between the USLE C-factor and CN2 in different land use categories offers insights into soil stability dynamics. Researchers utilize these factors to develop targeted strategies for sustainable land management [69]. In this study, the assigned C factor values for each LULC were rainforest (0.0002), pasture (0.0019), mangrove (0.0010), sugarcane (0.1), and urban area (0.2). These values have been recommended in various studies for hydrologically homogeneous basins in the same biome [70–72].

The results of this study indicated that CN values significantly affected the estimated streamflow and sediment production. CN2 emerges as one of the most sensitive parameters in determining the ratio of precipitation transformation into runoff. Several studies have consistently demonstrated that higher CN2 values correlate with increased runoff and peak flow in hydrological systems [73,74].

The model's performance was evaluated based on the overall hydrological behavior of the basin across all four flow measurement stations. Despite the limitations, the simulation results provided valuable insights into the effects of dynamic LULC input on the hydrological responses of this basin. However, it is important to note that the unsatisfactory performance in simulating streamflow and sediment yield can be partly attributed to the model's inability to accurately capture peak load events under high-flow conditions in similar basins, as reported in other studies [75]. Research conducted by [26] in the Pirapama River basin (from 1990 to 2001) has ascertained that erosive processes in the basin are influenced not merely by regional rainfall but also by factors such as slope, surface

roughness, soil types, and land uses. Specifically, areas with steeper slopes contribute more significantly to erosive processes compared to those with flatter terrains.

As anticipated, the results indicate an increase in streamflow and sediment yield associated with landscape modifications, specifically the reduction in forested areas and the expansion of agricultural lands. Despite incorporating dynamic LULC input, this study exhibits specific limitations encountered during the validation of streamflow and sediment yield. The uncertainty in observed data may have contributed to a slightly inferior model performance.

The SWAT model with dynamic LULC can be applied to various agricultural watersheds, both small and large scale, for more precise assessment and management of water quality and quantity. The current approach enables the study of the impacts of historical LULC changes on streamflow and sediment yield processes. The simulation results can be employed to inform the development of watershed management practices and the formulation of policies aimed at the sustainable management of watersheds and agriculture.

### *4.2. Impacts of LULC Changes on Sediment Yield*

With regard to sediment yield, it was observed that sub-basins with lower soil erosion rates are located upstream within the watershed. Conversely, higher sediment yields are predominantly found in the central upstream portions of the basin. Elevated levels in these regions are associated with land use, slope, and specific soil types, namely Argissols and Entisols. Predominant pasture usage, moderate slopes, and these soil types contribute to higher sediment yields. According to Serrão et al. [11], pastures, in comparison to forests, have a smaller leaf area index, shallower root zone, and elevated surface temperatures. These factors lead to reduced evapotranspiration and infiltration, thereby increasing surface runoff. Through the application of the SWAT model, Baker and Miller [76] demonstrated that changes in LULC in Kenya's Rift Valley resulted in a simultaneous increase in surface runoff, sediment yield, and a reduction in groundwater recharge.

Changes in land use and occupancy, resulting from human activities such as deforestation, reforestation, and urbanization, have a significant influence on the hydrological behavior of a watershed, particularly affecting surface runoff and erosive processes [77]. Forested areas, especially in tropical regions, play a critical role in attenuating peak streamflows during rainy seasons due to their low runoff coefficients and high rates of evapotranspiration [78]. In a study conducted by [79], it was noted that alterations in land use have a modulating effect on the hydrological cycle. Specifically, the increase in deforestation activities directly impacts both mean and peak streamflows.

Changes in land use have garnered increasing attention due to their potential environmental consequences, notably variations in sediment yield. These shifts directly affect the quality of water resources and have negative impacts on aquatic biodiversity and the overall health of aquatic ecosystems. Furthermore, elevated sediment production can lead to the siltation of rivers and lakes, impairing navigation and water infrastructure. To mitigate these effects, sustainable soil management practices, such as riparian vegetation conservation and conservation agriculture, are imperative. It is crucial to acknowledge the importance of interdisciplinary approaches to understand and address the complex interactions between land use and its environmental ramifications.

The results demonstrated that changes in LULC, when modeled using the SWAT, exhibited notable stability in flow and sediment yield variations. This suggests that factors such as geology and climate significantly influence the system's response, thereby mitigating the impact of land use changes. This phenomenon underscores the complexity of interactions within the hydrological cycle.

Recent research, such as those conducted by [80], suggests that geological, climatic, and hydrogeological factors can potentially overshadow the effects of changes in land use. In regions with resilient soils or dominant climatic conditions, alterations in agricultural practices may exert a relatively minor impact on hydrological responses. Additionally, soil characteristics, such as texture and structure, also play a pivotal role in modulating

changes in streamflow and soil erosion [81]. This observation underscores the importance of considering the intricate interplay between natural and anthropogenic factors in hydrological modeling studies. Under certain circumstances, soil conservation policies and agricultural practices may not yield the desired impact on erosion mitigation and flow regulation. Therefore, an integrated approach that accounts for multiple environmental factors is crucial for guiding effective decision-making in watershed management.

The introduction of dynamic LULC data enhanced the fidelity of the hydrological model, as it accounted for the temporal changes in LULC, thereby reflecting the complex hydro-sedimentological processes more accurately. The dynamic approach proved essential in capturing seasonal and annual variations, providing more precise insights into the hydrological behavior of the basin. Furthermore, it should be emphasized that the results obtained in this study highlight the importance of continually integrating dynamic LULC data to advance our understanding and efficient prediction of hydrological phenomena.

## 5. Conclusions

This study examined the influence of land use and occupancy trends on the hydrological balance and sediment yield within the Pirapama River basin. Overall, the accuracy analysis of the MapBiomas maps indicated high precision in classifications, exhibiting satisfactory and excellent percentages concerning producer accuracy, user accuracy, overall accuracy, and the Kappa index.

Trends in land use and occupancy showed that classes such as urban areas, pasture, water, and sugarcane have increased, whereas mangrove and rainforest areas have experienced a decline. These land use alterations have substantially impacted the hydrological balance in a wetland basin of the Atlantic Forest biome in Brazil.

With respect to the flow analysis for various scenarios, the results displayed minimal variation across simulations. This suggests that the examined land-use changes were insufficient to represent a discernable trend in either increased or decreased flow rates. Similarly, minimal variation was observed in the hydrological balance variables from one scenario to another, particularly for estimated values of surface runoff, percolation, and, most notably, evapotranspiration.

In the sub-basin surface runoff analysis, results exhibited more substantial variations in estimated rates but demonstrated similar behaviors across sub-basins from one scenario to another. Therefore, it was concluded that the observed changes in land use within the analyzed real-world scenarios did not directly and perceptibly influence the basin's hydrology for this region. However, the results concerning sediment yield estimates showed more significant variations between scenarios and among sub-basins, suggesting a possible influence of land use changes on the sedimentological dynamics of the basin, especially when compared to the variability of groundcover vegetation.

**Author Contributions:** Conceptualization, S.M.G.L.M.; data curation, J.F.d.S.V.; writing—original draft preparation, J.F.d.S.V.; writing—review and editing, R.S., C.A.G.S., M.M., A.M.K. and R.M.d.S.; visualization, C.A.G.S. and R.M.d.S.; supervision, S.M.G.L.M. All authors have read and agreed to the published version of the manuscript.

**Funding:** This study was also financed in part by the Brazilian Federal Agency for the Support and Evaluation of Graduate Education (Coordenação de Aperfeiçoamento de Pessoal de Nível Superior–CAPES)–Finance Code 001, and the National Council for Scientific and Technological Development, Brazil–CNPq (Grant No. 313358/2021-4, 309330/2021-1, and 420031/2021-9).

**Data Availability Statement:** The data presented in this study are available in this published paper.

**Conflicts of Interest:** The authors declare no conflict of interest.

## References

1. Loiselle, D.; Du, X.; Alessi, D.S.; Bladon, K.D.; Faramarzi, M. Projecting impacts of wildfire and climate change on streamflow, sediment, and organic carbon yields in a forested watershed. *J. Hydrol.* **2020**, *590*, 125403. [CrossRef]

2. Yin, S.; Gao, G.; Li, Y.; Xu, Y.J.; Turner, R.E.; Ran, L.; Wang, X.; Fu, B. Long-term trends of streamflow, sediment load and nutrient fluxes from the Mississippi River Basin: Impacts of climate change and human activities. *J. Hydrol.* **2023**, *616*, 128822. [CrossRef]
3. Juma, L.A.; Nkongolo, N.V.; Raude, J.M.; Kiai, C. Assessment of hydrological water balance in Lower Nzoia Sub-catchment using SWAT-model: Towards improved water governace in Kenya. *Heliyon* **2022**, *8*, e09799. [CrossRef] [PubMed]
4. Huq, E.; Abdul-Aziz, O.I. Climate and land cover change impacts on stormwater runoff in large-scale coastal-urban environments. *Sci. Total Environ.* **2021**, *778*, 146017. [CrossRef] [PubMed]
5. Wang, L.; Hou, H.; Li, Y.; Pan, J.; Wang, P.; Wang, B.; Chen, J.; Hu, T. Investigating relationships between landscape patterns and surface runoff from a spatial distribution and intensity perspective. *J. Environ. Manag.* **2023**, *325*, 116631. [CrossRef] [PubMed]
6. Rápalo, L.M.C.; Uliana, E.M.; Moreira, M.C.; da Silva, D.D.; Ribeiro, C.B.M.; da Cruz, I.F.; Pereira, D.R. Effects of land-use and -cover changes on streamflow regime in the Brazilian Savannah. *J. Hydrol. Reg. Stud.* **2021**, *38*, 100934. [CrossRef]
7. Zhao, C.S.; Yang, Y.; Yang, S.T.; Xiang, H.; Wang, F.; Chen, X.; Zhang, H.M.; Yu, Q. Impact of spatial variations in water quality and hydrological factors on the food-web structure in urban aquatic environments. *Water Res.* **2019**, *153*, 121–133. [CrossRef]
8. Zema, D.A.; Lucas-Borja, M.E.; Carrà, B.G.; Denisi, P.; Rodrigues, V.A.; Ranzini, M.; Arcova, F.C.S.; de Cicco, V.; Zimbone, S.M. Simulating the hydrological response of a small tropical forest watershed (Mata Atlantica, Brazil) by the AnnAGNPS model. *Sci. Total Environ.* **2018**, *636*, 737–750. [CrossRef]
9. Feitosa, T.B.; Fernandes, M.M.; Santos, C.A.G.; Silva, R.M.; Garcia, J.R.; Araujo Filho, R.N.; Fernandes, M.R.M.; Cunha, E.R. Assessing economic and ecological impacts of carbon stock and land use changes in Brazil's Amazon Forest: A 2050 projection. *Sustain. Produc. Consump.* **2023**, *41*, 64–74. [CrossRef]
10. Fonseca, C.A.B.; Al-Ansari, N.; Silva, R.M.; Santos, C.A.G.; Zerouali, B.; Oliveira, D.B.; Elbeltagi, A. Investigating relationships between runoff-erosion processes and land use and land cover using remote sensing multiple gridded datasets. *ISPRS Int. J. Geo-Inform.* **2022**, *11*, 272. [CrossRef]
11. Serrão, E.A.O.; Silva, M.T.; Ferreira, T.R.; de Ataide, L.C.P.; dos Santos, C.A.; de Lima, A.M.M.; da Silva, V.P.R.; de Sousa, F.A.S.; Gomes, D.J.C. Impacts of land use and land cover changes on hydrological processes and sediment yield determined using the SWAT model. *Int. J. Sedim. Res.* **2022**, *37*, 54–69. [CrossRef]
12. Senhorelo, A.P.; Sousa, E.F.; Santos, A.R.; Ferrari, J.L.; Peluzio, J.B.E.; Zanetti, S.S.; Carvalho, R.C.F.; Camargo Filho, C.B.; Souza, K.B.; Moreira, T.R.; et al. Application of the Vegetation Condition Index in the Diagnosis of Spatiotemporal Distribution of Agricultural Droughts: A Case Study Concerning the State of Espírito Santo, Southeastern Brazil. *Diversity* **2023**, *15*, 460. [CrossRef]
13. Venetsanou, P.; Anagnostopoulou, C.; Loukas, A.; Voudouris, K. Hydrological impacts of climate change on a data-scarce Greek catchment. *Theor. Appl. Climatol.* **2020**, *140*, 1017–1030. [CrossRef]
14. Trisurat, Y.; Sutummawong, N.; Roehrdanz, P.R.; Chitechote, A. Climate change impacts on species composition and floristic regions in Thailand. *Diversity* **2023**, *15*, 1087. [CrossRef]
15. Aloui, S.; Mazzoni, A.; Elomri, A.; Aouissi, J.; Boufekane, A.; Zghibi, A. A review of Soil and Water Assessment Tool (SWAT) studies of Mediterranean catchments: Applications, feasibility, and future directions. *J. Environ. Manag.* **2023**, *326 Pt B*, 116799. [CrossRef]
16. Dong, L.; Fu, S.; Liu, B.; Yin, B. Comparison and quantitative assessment of two regional soil erosion survey approaches. *Int. Soil Water Conserv. Res.* **2023**, *11*, 660–668. [CrossRef]
17. Osakpolor, S.E.; Kattwinkel, M.; Schirmel, J.; Feckler, A.; Manfrin, A.; Schäfer, R.B. Mini-review of process-based food web models and their application in aquatic-terrestrial meta-ecosystems. *Ecolog. Model.* **2021**, *458*, 109710. [CrossRef]
18. Coelho, A.J.P.; Matos, F.A.R.; Villa, P.M.; Heringer, G.; Pontara, V.; Almado, R.P.; Meira-Neto, J.A.A. Multiple drivers influence tree species diversity and above-ground carbon stock in second-growth Atlantic forests: Implications for passive restoration. *J. Environ. Manag.* **2022**, *318*, 115588. [CrossRef]
19. Ramos, E.A.; Nuvoloni, F.M.; Lopes, E.R.N. Landscape transformations and loss of Atlantic forests: Challenges for conservation. *J. Nat. Conserv.* **2022**, *66*, 126152. [CrossRef]
20. Silva, T.R.F.; Dos Santos, C.A.C.; Silva, D.J.F.; Santos, C.A.G.; Silva, R.M.; Brito, J.I.B. Climate Indices-Based Analysis of Rainfall Spatiotemporal Variability in Pernambuco State, Brazil. *Water* **2022**, *14*, 2190. [CrossRef]
21. Magarotto, M.G.; da Costa, M.F.; Tenedório, J.A.; Silva, C.P. Vertical growth in a coastal city: An analysis of Boa Viagem (Recife, Brazil). *J. Coast. Conserv.* **2016**, *20*, 31–42. [CrossRef]
22. Silva, R.M.; Santos, C.A.G. Aplicação do modelo hidrológico AÇUMOD baseado em SIG para a gestão de recursos hídricos do rio Pirapama. *Rev. Amb. Água* **2007**, *2*, 7–20. [CrossRef]
23. Woolhiser, D.A.; Smith, R.E.; Goodrich, D.C. *KINEROS, A Kinematic Runoff and Erosion Model: Documentation and User Manual*; ARS-77; U.S. Department of Agriculture, Agricultural Research Service: Washington DC, USA, 1990; 130p.
24. Arnold, J.G.; Srinivasan, R.; Muttiah, R.S.; Williams, J.R. Large area hydrologic modeling and assessment—Part I: Model development. *J. Am. Water Resour. Assoc.* **1998**, *34*, 73–89. [CrossRef]
25. Braga, A.C.F.M.; Silva, R.M.; Santos, C.A.G.; Galvão, C.O.; Nobre, P. Downscaling of a global climate model for estimation of runoff, sediment yield and dam storage: A case study of Pirapama Basin, Brazil. *J. Hydrol.* **2013**, *498*, 46–58. [CrossRef]
26. Viana, J.F.S.; Montenegro, S.M.G.L.; Silva, B.B.; Silva, R.M.; Srinivasan, R. SWAT parameterization for identification of critical erosion watersheds in the Pirapama River basin, Brazil. *J. Urban Environ. Eng.* **2019**, *13*, 42–58. [CrossRef]

27. Viana, J.F.S.; Montenegro, S.M.G.L.; Silva, B.B.; Silva, R.M.; Srinivasan, R.; Santos, C.A.G.; Araújo, D.C.S.; Tavares, C.G. Evaluation of gridded meteorological datasets and their potential hydrological application to a humid area with scarce data for Pirapama River basin, northeastern Brazil. *Theor. Appl. Climatol.* **2021**, *145*, 393–410. [CrossRef]
28. CPRH–Companhia Pernambucana de Meio Ambiente. Sistema de Informações Socioeconômicas da Bacia do Prapama. Recife: Companhia Pernambucana de Meio Ambiente. 1998. Available online: http://www.cprh.pe.gov.br/downloads/sisapmanual.pdf (accessed on 10 January 2023).
29. CPRH—Companhia Pernambucana de Meio Ambiente. *Diagnóstico Socioambiental do Litoral Sul de Pernambuco*; CPRH—Companhia Pernambucana de Meio Ambiente: Recife, Brazil, 2003.
30. Da Silva, R.M.; Montenegro, S.M.G.L.; Santos, C.A.G. Integration of GIS and remote sensing for estimation of soil loss and prioritization of critical sub-catchments: A case study of Tapacurá catchment. *Nat. Hazards* **2012**, *62*, 953–970. [CrossRef]
31. MapBiomas. Collection 4.0 of Brazilian Land Cover and Use Map Series. 2019. Available online: http://mapbiomas.org/en (accessed on 20 June 2023).
32. MapBiomas. Collection 4.0 of Brazilian Land Cover and Use Map Series: Accuracy Analysis. 2019. Available online: https://mapbiomas.org/en/accuracy-analysis (accessed on 20 June 2023).
33. Parente, L.; Ferreira, L.; Faria, A.; Nogueira, S.; Araújo, F.; Teixeira, L.; Hagen, S. Monitoring the Brazilian pasturelands: A new mapping approach based on the Landsat 8 spectral and temporal domains. *Int. J. Appl. Earth Obs. Geoinf.* **2017**, *62*, 135–143. [CrossRef]
34. Anderson, J.R.; Hardy, E.E.; Roach, J.T.; Witmer, R.E. A land use and land cover classification system for use with remote sensor data. *Geol. Surv. Prof. Pap.* **1976**, *964*, 34.
35. Congalton, R.G.; Green, K.; Group, F.; Raton, B. Assessing the accuracy of remotely sensed data—Principles and practices. *Int. J. Appl. Earth Obs. Geoinf.* **2009**, *11*, 448–449.
36. Mann, H.B. Nonparametric tests against trend. *Econometrica* **1945**, *13*, 245–259. [CrossRef]
37. Kendall, M.G. *Rank Correlation Methods*; Griffin: London, UK, 1975.
38. Pettitt, A.N. A Non-Parametric Approach to the Change-Point Problem. *J. R. Stat. Soc.* **1979**, *28*, 126–135. [CrossRef]
39. Sen, P.K. Estimates of the regression coefficient based on Kendall's tau. *J. Am. Stat.* **1968**, *63*, 1379–1389. [CrossRef]
40. Shannon, C.E.; Weaver, W. *The Mathematical Theory of Communication*; The University of Illinois Press: Urbana, IL, USA, 1964.
41. Simpson, E. Measurement of diversity. *Nature* **1949**, *163*, 688. [CrossRef]
42. Pielou, E.C. Species-diversity and pattern-diversity in the study of ecological succession. *J. Theor. Biol.* **1966**, *10*, 370–383. [CrossRef] [PubMed]
43. Arnold, J.G.; Allen, P.M.; Bernhardt, G. A comprehensive surface-groundwater flow model. *J. Hydrol.* **1993**, *142*, 47–69. [CrossRef]
44. APAC—Agência Pernambucana de Águas e Climas. *Pernambuco State Water Resources Status Report 2011/2012*; APAC—Agência Pernambucana de Águas e Climas: Recife, Brazil, 2013.
45. ANA—Agência Nacional de Águas. Portal HidroWeb. 2023. Available online: https://www.snirh.gov.br/hidroweb (accessed on 12 January 2023).
46. INMET—Instituto Nacional de Meteorologia. Banco de Dados Meteorológicos. 2023. Available online: https://bdmep.inmet.gov.br (accessed on 12 January 2023).
47. Abbaspour, K.C.; Yang, J.; Maximov, I.; Siber, R.; Bogner, K.; Mieleitner, J.; Zobrist, J.; Srinivasan, R. Modelling hydrology and water quality in the pre-alpine/alpine Thur watershed using SWAT. *J. Hydrol.* **2007**, *333*, 413–430. [CrossRef]
48. Rouholahnejad, E.; Abbaspour, K.C.; Vejdani, M.; Srinivasan, R.; Schulin, R.; Lehmann, A. A parallelization framework for calibration of hydrological models. *Environ. Model. Softw.* **2012**, *31*, 28–36. [CrossRef]
49. Nash, J.E.; Sutcliffe, J.V. River flow forecasting through conceptual models part I: A discussion of principles. *J. Hydrol.* **1970**, *10*, 282–290. [CrossRef]
50. Moriasi, D.N.; Arnold, J.G.; Van Liew, M.W.; Bingner, R.L.; Harmel, R.D.; Veith, T.L. Model evaluation guidelines for systematic quantification of accuracy in watershed simulations. *Trans. Am. Soc. Agric. Biol. Eng.* **2007**, *50*, 885–900.
51. Beltrão, J.A.; Da Silva, R.M.; Santos, C.A.G.; Dantas, J.C. Hydrological simulation in a tropical humid basin in the Cerrado biome using the SWAT model. *Hydrol. Res.* **2018**, *49*, 908–923.
52. Abe, C.A.; Lobo, F.L.L.; Dibike, Y.B.; Costa, M.P.F.; Santos, V.; Novo, E.M.L.M. Modelling the effects of historical and future land cover changes on the hydrology of an Amazonian Basin. *Water* **2018**, *10*, 932. [CrossRef]
53. Hernandes, T.A.D.; Scarpare, F.V.; Seabra, J.E.A. Assessment of the recent land use change dynamics related to sugarcane expansion and the associated effects on water resources availability. *J. Clean. Produc.* **2018**, *197*, 1328–1341. [CrossRef]
54. Op de Hipt, F.O.; Diekkrüger, B.; Steup, G.; Yira, Y.; Hoffmann, T.; Rode, M.; Näschen, K. Modeling the effect of land use and climate change on water resources and soil erosion in a tropical West African catchment (Dano, Burkina Faso) using SHETRAN. *Sci. Total Environ.* **2019**, *653*, 431–445. [CrossRef] [PubMed]
55. Wang, X.; Xin, L.; Tan, M.; Li, X.; Wang, J. Impact of spatiotemporal change of cultivated land on food-water relations in China during 1990–2015. *Sci. Total Environ.* **2020**, *716*, 137119. [CrossRef] [PubMed]
56. Serrão, E.A.O.; Silva, M.T.; Sousa, F.A.S.; Ataide, L.C.P.; Santos, C.A.; Silva, V.P.R.; Silva, B.K.N. Influence of land use and land cover on spatial and temporal variability of evapotranspiration in southeastern Amazonia, using the SWAT model. *Rev. Ibero-Amer. Ciênc. Amb.* **2019**, *10*, 134–148.
57. Oliveira, V.A.; Mello, C.R.; Viola, M.R.; Srinivasan, R.S. Land-use change impacts on the hydrology of the upper Grande River basin, Brazil. *Cerne* **2018**, *24*, 334–343. [CrossRef]

58. Serrão, E.A.O.; Silva, M.T.; Ferreira, T.R.; Silva, V.P.R.; Sousa, F.S.; Lima, A.M.M.; Ataide, L.C.P.; Wanzeler, R.T.S. Land use change scenarios and their effects on hydropower energy in the Amazon. *Sci. Total Environ.* **2020**, *744*, 140981. [CrossRef]
59. Silva, V.P.R.; Silva, M.T.; Braga, C.C.; Singh, V.P.; Souza, E.P.; Sousa, F.A.S.; Holanda, R.M.; Almeida, R.S.R.; Braga, A.C.R. Simulation of stream flow and hydrological response to land-cover changes in a tropical river basin. *Catena* **2020**, *162*, 166–176. [CrossRef]
60. Hussein, E.A.; Abd El-Ghani, M.M.; Hamdy, R.S.; Shalabi, L.F. Do anthropogenic activities affect floristic diversity and vegetation structure more than natural soil properties in hyper-arid desert environments? *Diversity* **2021**, *13*, 157. [CrossRef]
61. Castello, L.; McGrath, D.G.; Hess, L.L.; Coe, M.T.; Lefebvre, P.A.; Petry, P.; Macedo, M.N.; Renó, V.F.; Arantes, C.C. The vulnerability of Amazon freshwater ecosystems. *Conserv. Lett.* **2013**, *6*, 217–229. [CrossRef]
62. Guse, B.; Pfannerstill, M.; Fohrer, N. Dynamic modelling of land use change impacts on nitrate loads in rivers. *Environ. Process.* **2015**, *2*, 575–592. [CrossRef]
63. Sampaio, G.; Nobre, C.; Costa, M.H.; Satyamurty, P. Regional climate change over eastern Amazonia caused by pasture and soybean cropland expansion. *Geophys. Res. Lett.* **2017**, *34*, 1–7. [CrossRef]
64. Souahi, H.; Gacem, R.; Chenchouni, H. Variation in Plant Diversity along a Watershed in the Semi-Arid Lands of North Africa. *Diversity* **2022**, *14*, 450. [CrossRef]
65. Silva, R.M.; Santos, C.A.G.; Silva, V.C.L.; Medeiros, I.C.; Moreira, M.; Real, J.C. Effects of scenarios of land use on runoff and sediment yield for Cobres River basin, Portugal. *Geociências* **2016**, *35*, 609–622.
66. Sparovek, G.; Schnug, E. Soil tillage and precision agriculture: A theoretical case study for soil erosion control in Brazilian sugar cane production. *Soil Tillage Res.* **2001**, *61*, 47–54. [CrossRef]
67. SCS. *Hydrology, National Engineering Handbook, Supplement A, Section 4, Chapter 10*; Soil Conservation Service, USDA: Washington, DC, USA, 1956.
68. Wischmeier, W.H.; Smith, D.D. Predicting rainfall erosion losses—A guide to conservation planning. In *U.S. Department of Agriculture, Agriculture Handbook 537*; Science and Education Administration: Hyattsville, MD, USA, 1978.
69. Singh, A.; Jha, S.K. Identification of sensitive parameters in daily and monthly hydrological simulations in small to large catchments in Central India. *J. Hydrol.* **2021**, *601*, 126632. [CrossRef]
70. Fukunaga, D.C.; Cecílio, R.A.; Zanetti, S.S.; Oliveira, L.T.; Caiado, M.A.C. Application of the SWAT hydrologic model to a tropical watershed at Brazil. *Catena* **2015**, *125*, 206–213. [CrossRef]
71. dos Santos, F.M.; Pelinson, N.S.; de Oliveira, R.P.; Di Lollo, J.A. Using the SWAT model to identify erosion prone areas and to estimate soil loss and sediment transport in Mogi Guaçu River basin in Sao Paulo State, Brazil. *Catena* **2023**, *222*, 106872. [CrossRef]
72. Possantti, I.; Barbedo, R.; Kronbauer, M.; Collischonn, W.; Marques, G. A comprehensive strategy for modeling watershed restoration priority areas under epistemic uncertainty: A case study in the Atlantic Forest, Brazil. *J. Hydrol.* **2023**, *617 Pt B*, 129003. [CrossRef]
73. Hachemaoui, A.; Elouissi, A.; Benzater, B.; Fellah, S. Assessment of the hydrological impact of land use/cover changes in a semi-arid basin using the SWAT model (case of the Oued Saïda basin in western Algeria). *Model. Earth Syst. Environ.* **2022**, *8*, 5611–5624. [CrossRef]
74. Palacios-Cabrera, T.; Valdes-Abellan, J.; Jodar-Abellan, A.; Rodrigo-Comino, J. Land-use changes and precipitation cycles to understand hydrodynamic responses in semiarid Mediterranean karstic watersheds. *Sci. Total Environ.* **2022**, *819*, 153182. [CrossRef] [PubMed]
75. de Medeiros, I.C.; da Costa Silva, J.F.C.B.; Silva, R.M.; Santos, C.A.G. Run-off-erosion modelling and water balance in the Epitácio Pessoa Dam river basin, Paraíba State in Brazil. *Int. J. Environ. Sci. Technol.* **2019**, *16*, 3035–3048. [CrossRef]
76. Baker, S.N.; Miller, T.J. Using the Soil and Water Assessment Tool (SWAT) to assess land use impact on water resources in an East African watershed. *J. Hydrol.* **2013**, *486*, 100–111. [CrossRef]
77. Hoeltgebaum, L.E.B.; Dias, N.L. Evaluation of the storage and evapotranspiration terms of the water budget for an agricultural watershed using local and remote-sensing measurements. *Agric. For. Meteorol.* **2023**, *341*, 109615. [CrossRef]
78. Tumsa, B.C.; Kenea, G.; Tola, B. The application of SWAT+ model to quantify the impacts of sensitive LULC changes on water balance in Guder catchment, Oromia, Ethiopia. *Heliyon* **2022**, *8*, e12569. [CrossRef]
79. Gura, D.; Semenycheva, I. Successional changes in vegetation communities near Mine Pits. *Diversity.* **2023**, *15*, 888. [CrossRef]
80. Kijowska-Strugała, M.; Bochenek, W. Land use changes impact on selected chemical denudation element and components of water cycle in small mountain catchment using SWAT model. *Geomorphology* **2023**, *435*, 108747. [CrossRef]
81. Lyu, Y.; Chen, H.; Cheng, Z.; He, Y.; Zheng, X. Identifying the impacts of land use landscape pattern and climate changes on streamflow from past to future. *J. Environ. Manag.* **2023**, *345*, 118910. [CrossRef]


**Disclaimer/Publisher's Note:** The statements, opinions and data contained in all publications are solely those of the individual author(s) and contributor(s) and not of MDPI and/or the editor(s). MDPI and/or the editor(s) disclaim responsibility for any injury to people or property resulting from any ideas, methods, instructions or products referred to in the content.